# DYNAMIC MODELING AND CONTROL OF HYBRID ELECTRIC VEHICLE WITH BATTERIES, ULTRACAPACITORS AND FUEL CELL

*M. Rajabzadeh[1], *S. M. T. Bathaee[1], *M. A. Golkar[1]

[1]K. N. Toosi University of Technology

* Authors' email: Mahdi_rajabzadeh@ee.kntu.ac.ir, bathaee@kntu.ac.ir, golkar@eetd.kntu.ac.ir

**ABSTRACT-**This paper investigates the hybrid power source (HPS) for vehicular applications and presents a new configuration combining a fuel cell (FC), a battery pack and an ultracapacitor (UC) bank to create a HPS. Although many researchers have studied various powertrain topologies, component sizes, and control strategies in Hybrid electric vehicles (HEVs), but it is necessary to perform a detailed nonlinear study of the HEV. The dynamic models of system and subsystems is considered to simulate and analyse the long-term behavior of the vehicle. The purpose of the model is to provide an in-depth analysis of sublevel components in the vehicle and loss analysis in power electronics devices in converters associated with these sublevel components. An advanced control strategy is used to manage the power flows of the proposed system. Simulation results of vehicle configuration are discussed. The simulation results show that the presented method is both satisfactory and consistent with expectation.

**Keywords:** Hybrid electric vehicle (HEV), Dynamic modeling, Ultracapacitor, Battery, Fuel Cell, Hybrid power source (HPS)

## 1 INTRODUCTION

The world's petroleum resources is estimated to be used up till 2060, if the consumption rates be as present. Besides, environmental and economic concerns are the other convincing motivation to develop clean, efficient, and sustainable vehicles for urban transportation [1].

Since the hybrid vehicles consumes different types of fuel, there are many profits for them such as emission reduction, performance improvements and efficiency increases. All features of hybrid electric vehicles (HEVs) depend on the capability of their energy storage system (ESS), which not only is utilized to store large amounts of energy but also should be able to release it quickly according to load demands [2].

The development of hybrid electric vehicles (HEV) which utilize electrical power to drive automotive subsystems has taken on an accelerated pace [3-4]. Recent progresses in the areas of power electronics, electric motor drives, and control systems provides a motivation to improve the performance of electrical traction systems and their reliability [5].

Fuel cells (FCs) have significant features in generating reliable and efficient electrical power at steady state condition. Proton exchange membrane FCs (PEMFCs) with higher power density and low operation temperature are considered as the prime candidate for vehicle applications compared to other types of FCs [6-7].

Utilization of battery or ultracapacitor (UC) as energy storage can reduce the cost and improve the efficiency and performance of a FCHEV. UCs can store and deliver energy almost instantaneously. Therefore UCs are suitable in transient conditions such as startup, acceleration, sudden load changes and regenerative braking In contrast, batteries will experience high internal losses if they are discharged too quickly [8-9].

The voltage level and dynamic characteristic of the energy storage components are generally different from the desired energy sources, therefore the Power converters are needed to surmount the system improprieties [10-13]. The system is a multiconverter structure which shall be controlled simultaneously.

The optimal sizing and control strategies for FC/battery [14-17], FC/UC [16-19] and FC/battery/UC [20-21] vehicles have been studied. Most studies analyzed the component sizes and some also designed controller for HEV system.

In this paper, a dynamic model for a HEV with FC, battery and UC is developed and analyzed. It will provide a significant contribution to the field of the multisource system, particularly in nonlinear power electronics applications. In Section II, the structure and energy management of hybrid power source for vehicular applications are presented in detail. The dynamic system and subsystem modeling will be explained in detail in Section III. The simulation results and long term analysis for various conditions are presented in Section IV. The simulation results will show the system performance during a specific driving cycles. The waveforms that are obtained during the motor-drive cycle have shown the possibility of improving the performance of the whole system and validated the proposed control algorithms.

### Hybrid Power Source

The energy density, power density, lifetime, cost, and maintenance are the significant characteristics of ESSs. Batteries usually have high energy density and are capable of storing the mass of electric energy. However, UCs have high power density and fast response for charging/discharging during a long life cycle [22]. The FC is another clean and efficient power source; however, the slow dynamic of the FC limits its performance on transient conditions. At present, none of the mentioned devices could meet all requirements of HEVs [23].

### Source of the HPD

Various topologies can be utilized for HPS by combining various energy sources with different features. The main objectives of these combinations is to make HPS with high power and energy density. Bidirectional DC/DC converters are generally utilized for interface between battery/UC systems and DC bus, which enables both flow directions for charge and discharge [24]. Khaligh and et al has summarized structures, characteristics, and costs of ESS topologies for HEV, as well as comparisons of ESSs of typical market-available HEVs [25].

Principally, FC electrical characteristics need low-voltage high-current structures. A classical boost converter is a prime candidate for interface between FC and dc-link because it operates in the current control mode in a continuous condition. [26].

The FC operating constraints must be taken into consideration while controlling the boost converter to ensure

minor impact to the FC. The FC power must be retained within specific intervals. The FC current slope must be limited to avoid starvation phenomenon. The ripple of FC current must be limited to 5% of the nominal current and the switching frequency of the FC current must be greater than 1.25 kHz [27].

Bidirectional buck-boost converter enables the UC to store energy regenerative braking and release it transient condition such as startup, acceleration and hill climbing. The regenerative brake energy is to be captured without considering the efficiency, as this energy would otherwise spoiled and lost as heat in the friction brakes [28]. However, we are seeking for efficient EMS which leads to improved fuel efficiency for transient drive cycles.

The Proposed structure of FC/Battery/UC Hybrid Power Sources is shown in Fig. 1. The battery actual voltage curve is almost linear over its working range. There is no battery converter in this structure in order to improve system efficiency and converter cost. Then, this system will be operated based on unregulated dc bus voltage, in which the dc bus voltage is equal to the battery voltage.
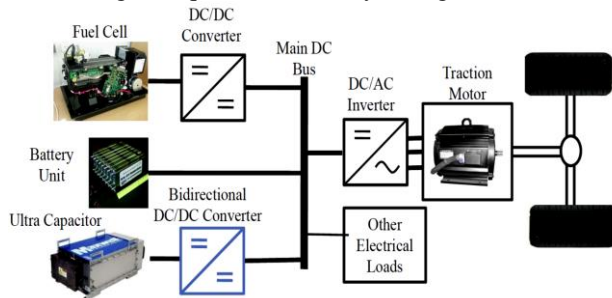


Fig. 1. Proposed structure of FC/Battery/UC HPS

## Energy management of the HPS

Energy management in HEVs allows the system to store the extra and reversible energy to ESS and deliver the energy to load at a different load condition. There are energy losses in Power converters and storage systems which an energy management system (EMS) should improve the fuel efficiency of the HEV. This will be done by shifting the operation of the fuel converter to an improved efficiency load condition by an amount sufficient to offset the losses of the energy storage and discharge processes.

The EMS of HPSs has already been investigated recently and some control strategies was presented. The problem of conventional controllers can be summarized as follows: Most of the conventional controllers are designed based on linear control theory and operates during a specific operating point so the definition of system states will be important. Transient and undefined conditions may lead to a phenomenon of chattering [29]. The control system proposed here is based on nonlinear control theory, thus, naturally, the problem of chattering would not happen here.

System and Subsytum Modeling
The HEV system is modeled dynamically based on each component dynamic model. Therefore the dynamic model of HPS and multiconverter structure is presented in this section.

## Fuel Cell Modeling

PEMFCs are the best candidate for vehicular application based on its specific features. Fig. 2 shows the cross section of a typical PEMFC. The hydrogen from the fuel source inters from the left side of the cell and while atmospheric

oxygen inters from the right side. On the left side of the cell, hydrogen converts to electrons and hydrogen ions in the presence of a catalyst. Combination of oxygen, electrons, and hydrogen ions on the right side of the cell, produce water and energy. The hydrogen side of catalyst is anode and the air side will be cathode. Thus, the definitions of the anode and cathode are reversed from the perspective of the electrical load, as positive electrical current flows from the cathode of the FC to the anode [30].
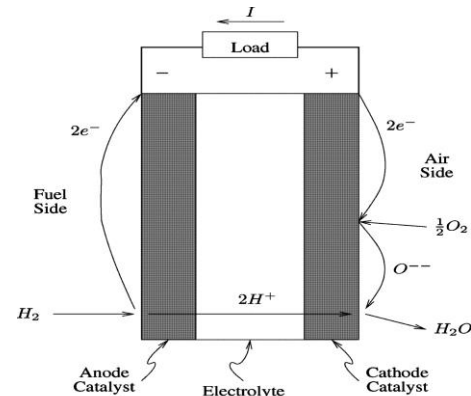


Fig. 2. Conceptual diagram of PEM hydrogen/oxygen FC

The produced voltage inside the cell ($E$) known as Nernst's instantaneous voltage may be expressed as follows:

$$E = N_0 \left[ E_0 + \frac{RT}{2F} \log \left[ \frac{p_{H_2} \sqrt{p_{O_2}}}{p_{H_2O}} \right] \right] \quad (1)$$

Where;

| | |
|---|---|
| $E$ | Nernst instantaneous voltage [V]; |
| $E_0$ | Standard no load voltage [V]; |
| $N_0$ | number of series FCs in the stack; |
| $F$ | Faraday's constant [C/kmol]; |
| $R$ | universal gas constant [(1 atm)/(kmol.K)]; |
| $T$ | Absolute temperature [K]; |
| $P_{H2}$ | Hydrogen partial pressure [atm]; |
| $P_{H2O}$ | Water partial pressure [atm]; |
| $P_{O2}$ | Oxygen partial pressure [atm]; |

The output voltage of cell is smaller than the inside voltage and there are activation and ohmic voltage drops. The following equations may defines the output voltage of cell:

$$V_{cell} = E - \eta_{act} - \eta_{ohm} \quad (2)$$

$$\eta_{act} = B \ln(CI'_{fc}) \quad (3)$$

$$\eta_{ohm} = R^{int} I'_{fc} \quad (4)$$

Where;

| | |
|---|---|
| $V_{cell}$ | DC output voltage of FC system [V]; |
| $\eta_{act}$ | Activation voltage drop [V]; |
| $\eta_{ohmic}$ | Ohmic voltage drop [V]; |
| $B, C$ | Constants; |
| $I'_{fc}$ | FC system feedback current [A]; |
| $R^{int}$ | FC internal resistance[$\Omega$]; |

## Batter Modeling

At present, the battery is still the most reliable and also expensive energy storage device for HPS. A pack of lithium-ion battery is considered for the HEV. In order to analyze the behavior of battery a dynamic model is required. The model is originated from experimental tests, where open circuit voltage (OCV) tests are performed on continuous discharge

of the battery, by the application of periodic current discharge. Therefore, the nonlinear RC models are developed to model nonlinear OCV characteristics of the battery [31]. The proposed nonlinear model is shown in Fig. 3.
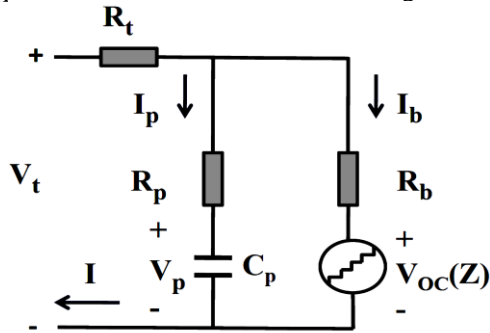


Fig. 3. Battery dynamic model structure

The terminal voltage equation is given as

$$V_t = IR_t + I_p R_p + V_p \tag{5}$$

$$V_t = IR_t + I_b R_b + V_{OC}(Z) \tag{6}$$

Where;

$V_t$        Terminal voltage [V];
$V_{OC}(Z)$   Nonlinear voltage source [V];
$Z(t)$      Battery state of charge (SOC);
$C_p$        Capacitance for polarization effect modeling [F];
$R_b$        Propagation resistor [Ω];
$R_p$        Diffusion resistor [Ω];
$R_t$        Ohmic resistance [Ω];
$I$          Instantaneous current (positive for charging, negative for discharging) [A].

The SOC is described as a proportion of the remaining capacity to the nominal capacity of the cell. The remaining capacity is equal to the number of ampere-hours that can be drawn from the cell at room temperature with the C/30 rate before it is fully discharged [32]. Therefore, the SOC can be defined as follows;

$$Z(t) = Z(0) + \int_0^t \frac{I_b(\tau)}{C_n} d\tau \tag{7}$$

Where $C_n$ is the nominal capacitance of the cell.

**Ultracapacttor Modeling**
UCs can deliver and store energy almost instantaneously. The stored energy can be delivered to the DC-bus at nearly any discharge rate. The dynamic model of UC unit can be extracted from the RC equivalent circuit shown in Fig. 4. The model is consist of an ideal capacitor ($C$) connecting to the dielectric leakage resistance ($R_P$) in parallel and the whole circuit is connected in series to the equivalent series resistance ($R_S$) [33].
The terminal voltage of the UC cell ($V_t$) can be calculated via Kirchhoff's voltage and current laws as follows

$$V_t = iR_s - \left[ V_{C0} - \int_0^t \frac{i}{C} e^{t/R_p C} dt \right] e^{-t/R_p C} \tag{8}$$

The UC bank is composed of seven Modules based on Maxwell TECHNOLOGIES UCs BMOD0165 P048 BXX model in series. Each module is consisting of 18 UC cells connected in series.
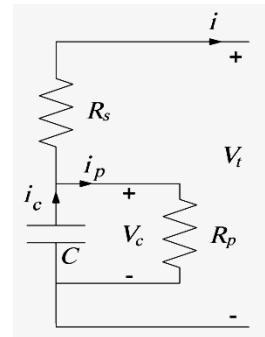


Fig. 4. Classical equivalent model for the UC unit

**Buck-Boost Converter (F Converter) Modeling**
A unidirectional DC/DC boost converter is utilized to adjust the low DC voltage of the FC to rated DC-link voltage and avoid the reverse current back to the FC. The power circuit of boost converter is shown in Fig. 5. The boost converter is consisted of a high frequency inductor $L_1$, equivalent series resistances $R_1$, an IGBT switch $S_1$, a diode $D_1$ and a capacitor $C_{dc}$ as an output filter. In order to protect the FC against overvoltage in transient condition an input capacitor $C_{fc}$ is added. A PWM controls the IGBT switch using $d_1$ signal which is one or zero. The converter model can be defined as the following state equation:

$$\frac{di_{fc}}{dt} = -(1-d_1)\frac{V_{dc}}{L_1} - \frac{R_1 i_{fc}}{L_1} + \frac{V_{fc}}{L_1} \tag{9}$$

$$\frac{dV_{dc}}{dt} = (1-d_1)\frac{i_{fc}}{C_{dc}} - \frac{i'_{fc}}{C_{dc}} \tag{10}$$

Where $i_{fc}$ and $i'_{fc}$ are the output current of FC circuit and converter respectively. $V_{fc}$ and $V_{dc}$ are the FC and DC-link voltage respectively. Note that the battery voltage $V_b$ is equal to DC-link voltage $V_{dc}$ ($V_{dc} = V_b$).
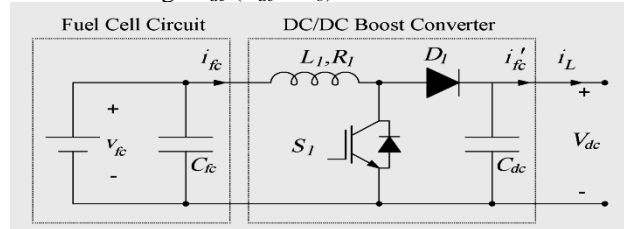


Fig. 5. Power circuit of boost converter

**Buck-Boost Converter (C Converter) Modeling**
The UC bank is connected to the DC-link using a bidirectional converter to ensure the charge and discharge of the electric power storage devices. Fig. 6 shows the power circuit of buck-boost converter. The converter is consisted of a high frequency inductor $L_2$, equivalent series resistances $R_2$, two IGBT switch $S_2$ and $S_3$. The IGBT switches are controlled by two binary signals $d_2$ and $d_3$. During boost operating mode (discharge mode), $S_2$ is on, and $S_3$ is off, and the UC module provides energy to the DC-link ($i_{uc} > 0$). Contrary to boost mode, in buck operating mode, $S_3$ is on, and $S_2$ is off, and the UC module will be charged ($i_{uc} < 0$). The buck-boost converter model can be given by the following differential equations:

$$\frac{di_{uc}}{dt} = -\left[ k(1-d_2) + (1-k)d_3 \right]\frac{V_{dc}}{L_2} - \frac{R_2 i_{uc} + V_{uc}}{L_2} \tag{11}$$

$$i'_{uc} = \left[ k(1-d_2) + (1-k)d_3 \right] i_{uc} \tag{12}$$

Where $k=1$ in boost mode and $k=0$ in buck mode. A new parameter $d_{23}$ can be defined as virtual control signal for buck-boost converter as bellow:

$$d_{23} = \left[ k(1-d_2) + (1-k)d_3 \right] \qquad (13)$$
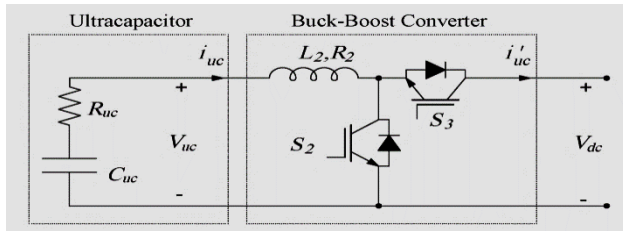


Fig. 6. Power circuit of buck-boost converter

## Overall System Modeling

The following equation achieves by exerting Kirchhoff's current law at DC bus node.

$$i_{fc}' + i_{uc}' + i_b = i_L \qquad (14)$$

$$i_{fc}' = i_L - i_b - d_{23}i_{uc} \qquad (15)$$

Where $i_b$ and $i_L$ are the battery and load currents respectively. The overall system differential equations will be arisen from (9), (10), (11) and (15) as follows:

$$\frac{di_{fc}}{dt} = -(1-d_1)\frac{V_b}{L_1} - \frac{R_1 i_{fc}}{L_1} + \frac{V_{fc}}{L_1} \qquad (16)$$

$$\frac{di_{uc}}{dt} = -d_{23}\frac{V_b}{L_2} - \frac{R_2}{L_2}i_{uc} + \frac{V_{uc}}{L_2} \qquad (17)$$

$$\frac{dV_b}{dt} = (1-d_1)\frac{i_{fc}}{C_{dc}} + \frac{d_{23}i_{uc}}{C_{dc}} + \frac{i_b}{C_{dc}} - \frac{i_L}{C_{dc}} \qquad (18)$$

The main objective is to establish the dynamic control strategy of the DC/DC converters for energy management between the batteries and UCs. This dynamic control strategy is based on current control because the DC-link voltage level is imposed by the battery module.

## SIMULATION RESULTS AND ANALYSIS

The dynamic model of an HEV system has been implemented in the MATLAB/Simulink environment. The performance of the proposed energy management and control system is demonstrated by means of numerical simulations. The specifications of a sample vehicle and all the individual components are summarized in Table 1.

The FCEV is simulated under a driving cycle which is shown in Fig. 7. The vehicle must track the driving cycle. It is assumed that the efficiency of power inverter is equal to 75% and the value of DC bus voltage is 300 V.

The simulation results focus on the dynamic behavior of HEV system and the losses in the subsystems. The HPS is combination of FC, battery and UC. The behavior of the HEV traction system and induction motor are given in Fig. 7. It shows vehicle speed; gear setting; the rotational speed of the induction motor; the actual induction motor torque and the load current respectively. Here shifting of gears is clearly visible in motor speed by short-term accelerations and decelerations and again is obvious as large spikes in the torque.

The time constants associated with the FC are much slower than those of the traction system. Thus, the behavior of most

of the FC signals will be slower and closer to an average value.

Fig. 8 shows a collection of graphs from the HEV subsystems. The output current of the FC going into the dc/dc boost converter, where the transients of this current are slow compared to the induction machine load current, giving an average of the required load current.

**Table 1. Specifications of vehicle and the components**

| | Subject | Quantity |
|---|---|---|
| Vehicle | Overall Vehicle Mass | 1922 kg |
| | Maximum Speed | 120 km/h |
| | Acceleration 0-100 km/h | 12.5sec |
| | Rolling Resistance Coefficient | 0.01 |
| | Aerodynamic Drag Coefficient | 0.3 |
| | Front Area | 2.5 m² |
| Induction Machine | Nominal Power | 37 kW |
| | Peak Power | 46.25 kW |
| | Maximum Speed | 120 rpm |
| | Maximum Torque | 255 Nm |
| PEMFC | Nominal Voltage | 42 V |
| | Nominal Current | 520 A |
| | Maximum Power | 22 kW |
| | Output Capacitor $C_{fc}$ | 1.66 mF |
| Battery | Capacity | 28.26 MJ |
| | Resistance (ESR) $R_t$ | 33 mΩ |
| | Nominal Voltage $U_{uc}$ | 300 V |
| UC | Equivalent Capacity $C_{uc}$ | 50 F (3.2 MJ) |
| | Resistance (ESR) $R_{uc}$ | 44.1 mΩ |
| | Nominal Voltage $U_{uc}$ | 250 V |
| Converters | Inductance, $L_1$ and $L_2$ | 3.3 mH |
| | Inductances ESR, $R_1$ and $R_2$ | 20 mΩ |
| | DC-Link Filtering Capacitor $C_{dc}$ | 1.66 mF |
| | Switching Frequency, $f_s$ | 15 kHz |

The evolution of the battery charge SOC and the UC SOC during the drive cycle can also be seen in Fig. 8. It can be noticed that the fluctuations of UC charge is more than the battery charge due to its smaller capacity. Thus, with an UC, the system is significantly more efficient. The battery capacity is larger than needed for this cycle, thus the short-term changes in the battery charge are only a few percent. The associated battery and dc-bus voltage are also shown in Fig. 8. Notice that the battery voltage range is narrow because the SOC is changing only slightly. However, the bus voltage drops significantly every time the vehicle accelerates and increases when the vehicle regenerates. This is related to battery resistance and the small bus capacitance. It is evident that the buck-boost converter between the UC and the dc-bus can enforce near-constant bus voltage.

In general, the battery/FC/UC hybrid has better performance than the other hybrid sources, because the UC can more effectively assist the FC to meet the transient power demand where high-current charges and discharges from the battery will reduce its lifetime as well.

Load or regeneration spikes translate into fast discharges of the battery and result in substantial loss. Although there is some uncertainty due to the low UC ESR, the losses in the UC module are more than in the battery module. But when power is cycled quickly, the battery experiences high losses, while the losses in the UC are much lower.

The simulation can be checked with a power balance. The values of the average power production and consumption in the HEV with the FC, battery and UC are given in Table 2.

**Table 2. Power Balance of HEV Model**

| Power | Battery (W) | UC (W) | FC (W) | Vehicle system (W) | Total (W) |
|---|---|---|---|---|---|
| produced | 2608 | 28 | 1266 | ---- | 3902 |
| consumed | 1431 | 235 | 99 | 2094 | 3859 |
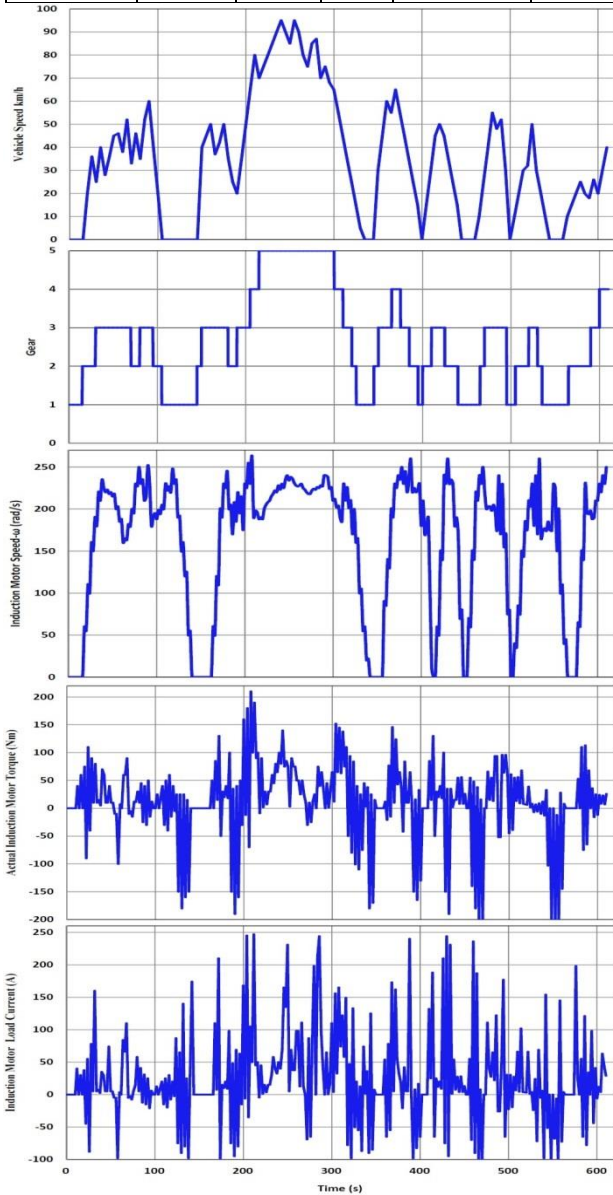


**Fig. 7. Vehicle speed; gear setting; the induction motor speed; the actual induction motor torque and the dc-bus load current.**

Average power produced in the system must equal consumed average power plus any change in stored energy. The average power produced by the FC for this test run is 1266 W. The battery is discharged by 4.7%, corresponding to an average power of 2.608 kW. The 0.72% charge decrease in the UC corresponds to an average power production of 28 W, resulting in a total average power production of 3.9 kW. The average power consumption of the traction system is 2.094 kW, and the average losses in the battery and the FC dc/dc converter are 1431 W and 99 W, respectively. The losses in the UC module are 235 W, considerably lower than the battery losses. The total average power consumption is about 3.859 kW very close to the average power production.

The small difference between production and consumption is

a computational limit consisted of uncertainties in the model and parameters. Some of the uncertainty factors in this simulation are the FC model, its parameters and the battery parameters, which were approximated from actual measurements.
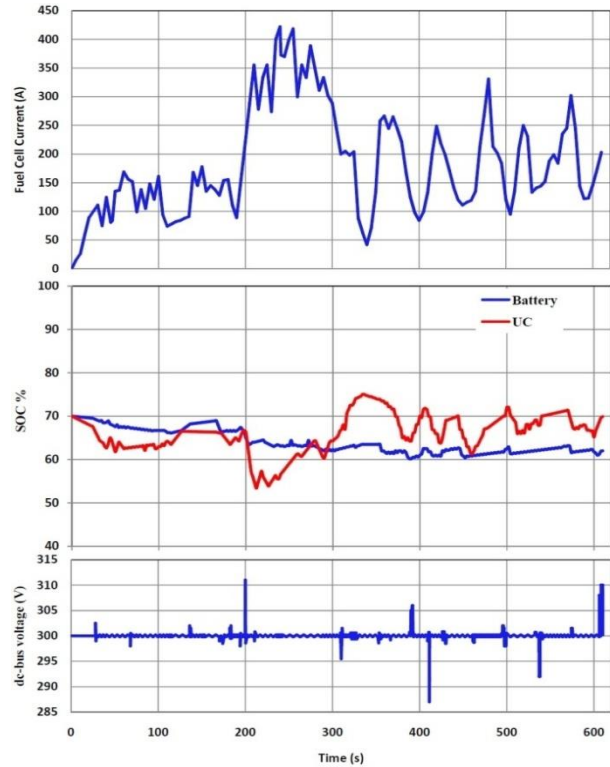


**Fig. 8. FC current; SOC of battery and UC; dc-bus voltage**

## CONCLUSION

Many works have been developed in recent years in the field of design and analysis of hybrid electric vehicles and support comparisons over long drive cycles. In the past, dynamic simulation models have focused mainly on the analysis of control strategies. In this paper, HPS for HEVs is investigated by considering the characteristics of the components. The HPS is consisted of FC, UC bank and battery pack to achieve both high power density and high energy density which means the combination of fast response sources and slow dynamic sources. The advantages of HPS could include improved vehicle performance and fuel economy and lower system cost. A boost dc/dc converter and a buck-boost converter are utilized to connect the HPS to dc bus. This paper presents a dynamic model for HEV system consisting of the dynamic model of HPS components and multiconverter structure. The proposed dynamic simulation system for an HEV is implemented in Matlab/Simulink. The purpose of the model is to provide an in-depth analysis of sublevel components in the vehicle and loss analysis in power electronics devices in converters associated with these sublevel components. The focus of the model is a detailed assessment of different subsystem components. Simulation results of vehicle configuration are discussed.

The simulation results show that the presented method is both satisfactory and consistent with expectation.

**REFERENCES**:

[1] Husain, I., *Electric and Hybrid Vehicles Design Fundamentals*, Taylor & Francis e-Library (2005)

[2]  Lukic, S., J. Cao, R. C. Bansal, F. Rodriguez, and A. Emadi, "Energy storage systems for automotive applications," *IEEE Transaction on Industrial Electronic,* **55**(6): 2258–2267(2008).

[3]  Chan, C. C. and Y. S. Wong, Electric vehicles charge forward, *IEEE Power and Energy Magazine,* **2**(6): 24–33(2004)

[4]  Hoelscher, D., A. Skorez, Y. Gao, and M. Ehsani, "Hybridized electric energy storage systems for hybrid electric vehicles," *IEEE Vehicle Power Propulsion Conference,* 1–6(2006)

[5]  Emadi, A., A. Khaligh, C. H. Rivetta and G. A. Williamson, "Constant Power Loads and Negative Impedance Instability in Automotive Systems: Definition, Modeling, Stability, and Control of Power Electronic Converters and Motor Drives" *IEEE Transaction on Vehicular Technology,* **55**(4): 1112–1125(2006).

[6]  Thounthong, P., B. Davat, and S. Raël, "Drive friendly," *IEEE Power and Energy Magazine*, **6**(1): 69–76(2008).

[7]  Rajashekara, K., "Hybrid fuel cell power in aircraft," *IEEE Industrial Application Magazine*, **14**(4): 54–60(2008).

[8]  Pukrushpan, J.T., H. Peng, and A.G. Stefanopuolou, "Control-oriented modeling and analysis for automotive fuel cell system," *Journal of Dynamic Systems, Measurement, and Control*, **126**(1): 14–25(2004).

[9]  Emadi, A., K. Rajashekara, S.S. Williamson and S.M. Lukic, "Topological overview of hybrid electric and fuel cell vehicular power system architectures and configurations," *IEEE Transaction on Vehicular Technology,* **54**(3): 763–770(2005).

[10] Moreno, J., M. E. Ortuzar, and J. W. Dixon, "Energy management system for a hybrid electric vehicle, using ultracapacitors and neural networks," *IEEE Transaction on Industrial Electronic,* **52**(2): 614–623(2006).

[11] Musardo, C., G. Rizzoni, and B. Staccia, "A-ECMS: An adaptive algorithm for hybrid electric vehicle energy management," *IEEE CDC-ECC, Seville, Spain,* 1816–1823(2005)

[12] Gao Y., and M. Ehsani, "Parametric design of the traction motor and energy storage for series hybrid off-road and military vehicles," *IEEE Transaction on Power Electronic,* **21**(3): 749–756(2006).

[13] Atwood, P., S. Gurski, D. J. Nelson, and K. B. Wipke, "Degree of hybridization modeling of a fuel cell hybrid electric sport utility vehicle," *SAE International Journal of Engines,* **110**: 93–100(2001)

[14] Kim M. J. and H. Peng, "Combined control/plant optimization of fuel cell hybrid vehicles," *American Control Conference, Minneapolis,* 496–501(2006).

[15] Paganelli, G., Y. Guezennec, and F. Rizzoni, "Optimizing control strategy for hybrid fuel cell vehicle," *the SAE World Conference., Detroit,* (2002)

[16] Gao, W., "Performance comparison of a fuel cell-battery hybrid powertrain and a fuel cell–ultracapacitor hybrid powertrain," *IEEE Transaction on Vehicular Technology,* **54**(3): 846–855(2005).

[17] Rousseau, A., P. Sharer, and R. Ahluwalia, "Energy storage requirements for fuel cell vehicles," *the SAE World Conference., Detroit* (2004).

[18] Schiffer, J., O. Bohlen, R. W. De Doncker, D. U. Sauer, and A. K. Young, "Optimized energy management for fuel cell–supercap hybrid electric vehicles," *IEEE Vehicular Power Propulsion Conference, Chicago, IL,* 341–348(2005).

[19] Wu Y., and H. Gao, Optimization of fuel cell and supercapacitor for fuel-cell electric vehicles, *IEEE Transaction on Vehicular Technology,* **55**(6): 1748–1755(2006).

[20] Schupbach R., and J. Balda, "The role of ultracapacitors in an energy storage unit for vehicle power management," *IEEE Vehicular Technology Conference, Orlando, FL,* 3236–3240(2003).

[21] Pede, G., A. Iacobazzi, S. Passerini, A. Bobbio, and G. Botto, "FC vehicle hybridisation: An affordable solution for an energy-efficient FC powered drive train," *Journal of Power Sources,* **125**(2): 280–291(2004).

[22] Lu, Y., H. Hess, and D. Edwards, "Adaptive control of an Ultracapacitor energy storage system for hybrid electric vehicles," *IEEE Electric Machine Drives Conference,* **1**: 129–133(2007).

[23] Williamson, S., A. Khaligh, S. Oh, and A. Emadi, "Impact of energy storage device selection on the overall drive train efficiency and performance of heavy-duty hybrid vehicles," IEEE Vehicle Power Propulsion *Conference*, Sep. 381–390(2005).

[24] Bauman J., and M. Kazerani, "A Comparative Study of Fuel-Cell–Battery, Fuel-Cell–Ultracapacitor, and Fuel-Cell–Battery–Ultracapacitor Vehicles" *IEEE Transaction on Vehicular Technology,* **57**(2): 760-769(2008).

[25] Khaligh, A., and Z. Li, Battery, "Ultracapacitor, Fuel Cell, and Hybrid Energy Storage Systems for Electric, Hybrid Electric, Fuel Cell, and Plug-In Hybrid Electric Vehicles: State of the Art" *IEEE Transaction on Vehicular Technology,* **59**(6): 2806–2814 (2010).

[26] Thounthong, P., V. Chunkag, P. Sethakul, Be. Davat, and M. Hinaje, "Comparative Study of Fuel-Cell Vehicle Hybridization with Battery or Supercapacitor Storage Device" *IEEE Transaction on Vehicular Technology,* **58**(8): 3892-3904(2008).

[27] Thounthong, P., B. Davat, S. Raël, and P. Sethakul, Fuel cell highpower applications, *IEEE Industrial Electronic Magazine,* **3**(1):3, 32–46(2009).

[28] Lai J. and D. J. Nelson, "Energy Management Power Converters in Hybrid Electric and Fuel Cell Vehicles" *Proceedings of the IEEE conference,* **95**: 766-777(2007).

[29] Sadli, I., P. Thounthong, J. P. Martin, S. Raël, and B. Davat, "Behavior of a PEMFC supplying a low voltage static converter," *Journal of Power Sources*, **156**(1): 119–125(2006).

[30] Pasricha S. and S. R. Shaw, "A Dynamic PEM Fuel Cell Model" *IEEE Transaction on Energy Conversion,* **21**(2): 484-491(2006).

[31] Kim, S. "Nonlinear State of Charge Estimator for Hybrid Electric Vehicle Battery" *IEEE Transaction on Power Electronic*, **23**(4): 2027-2034(2008).

[32] Fuel Cell Handbook, 5th ed. *EGG Services Parsons Inc.*, U.S. Department of Energy, (2000).

[33] Uzunoglu, M. and M. S. Alam, "Dynamic Modeling, Design, and Simulation of a Combined PEM Fuel Cell and Ultracapacitor System for Stand-Alone Residential Applications," *IEEE Transaction on Energy Conversion,* **21**(3): 767-775(2006).